THE DESIGN OF AN AIRFOIL FOR A HIGH-ALTITUDE, LONG-ENDURANCE REMOTELY PILOTED VEHICLE

Mark D. Maughmer
The Pennsylvania State University
University Park, Pennsylvania

Dan M. Somers
NASA Langley Research Center
Hampton, Virginia

AIRFOIL/AIRCRAFT DESIGN INTEGRATION

Whereas the airfoil to be used on a new aircraft was once chosen from a catalog of possibilities as the compromise which most closely matched the design requirements, the state of airfoil design is now at such a level that each new vehicle should have an airfoil tailored specifically to the intended mission. The role of the airfoil designer in this case is as it has always been, that is, to achieve the required lift for the least possible drag. It should not be inferred, however, that the best airfoil design is accomplished by maximizing the section lift-to-drag ratio. Instead, by making use of modern airfoil design technologies, the designer arrives at the most suitable airfoil for a particular aircraft by trading off the conflicting goals of achieving low section profile-drag coefficients through laminar-flow management, for example, against attaining high maximum lift coefficients which reduce the wetted-area drag by allowing a reduction in the required wing area. These types of trade-offs make it clear that in order to achieve the highest levels of aircraft performance possible, the airfoil design process should be integrated, as shown in the flow diagram of Fig. 1, with that of the aircraft. In tailoring the airfoil to match the aircraft, the most significant element in this diagram is the airfoil/aircraft design iteration loop. Clearly, the more closely the baseline airfoil data used in the preliminary design process match the mission requirements, the fewer the iterations necessary in the design loop.

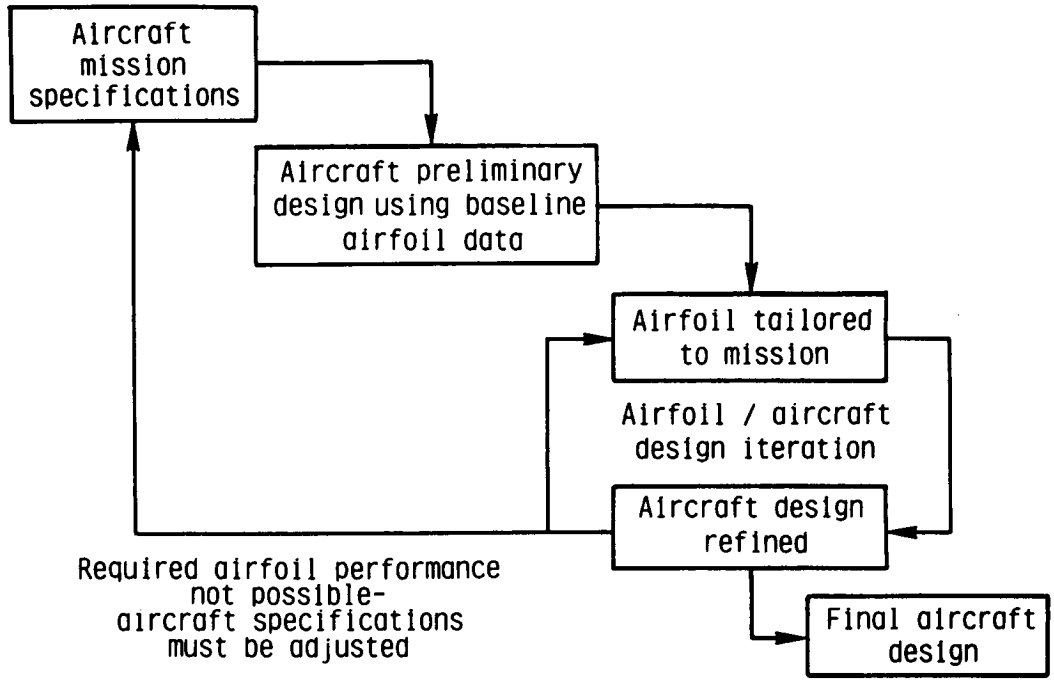

Figure 1

TYPICAL SPECIFICATIONS FOR A HIGH-ALTITUDE, LONG-ENDURANCE REMOTELY PILOTED VEHICLE

Currently, there is interest in the development of high-altitude, long-endurance remotely piloted vehicles for a number of proposed missions, including communications relaying, weather monitoring, and providing cruise missile targeting information. The preliminary design and sizing of such vehicles is complicated however, by the fact that data regarding suitable airfoils are limited. This is due to the fact that such vehicles, unlike those for which the majority of airfoils have been developed in the past, operate at fairly high lift coefficients and at relatively low Reynolds numbers. Thus, to provide realistic airfoil performance information for preliminary design purposes, a generic airfoil has been designed for the aircraft having the specifications given in Fig. 2. These specifications are representative of the aircraft proposed for the missions noted.

Wing span = 25m (82 ft)

Gross weight = 2000 kg (4400 lbs)

Empty weight = 1000 kg (2200 lbs)

Payload = 150-500 kg (330-1100 lbs)

Operational altitude = 20,000 m (66,000 ft)

Endurance ≈ 90 hrs.

Range ≈ 32,000 km (20,000 mi)

Figure 2

DESIGN GOALS

Based on performance studies of the aircraft having the specifications given in Fig. 2, the airfoil design requirements for the section located at the mean aerodynamic chord emerged. These requirements are summarized in the form of the section drag polar presented in Fig. 3. The design goal is to achieve the lift coefficients required for the key operational points noted in the figure, and to achieve them with the lowest possible profile-drag coefficients. Thus, the desired polar is of the form shown, but moved to the left as far as possible for the given width of the laminar "bucket". In addition, subject to the other design constraints, it is desirable to achieve a reasonably high maximum lift coefficient for take-off and landing performance.

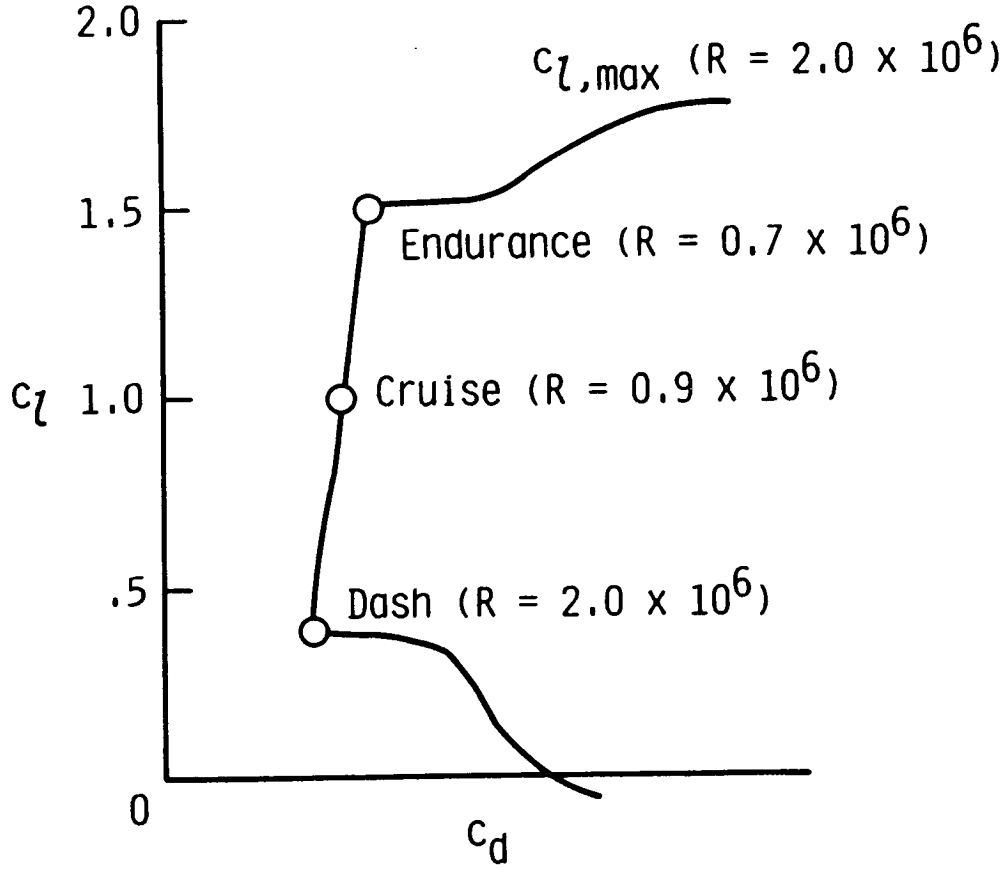

Figure 3

FIGURE OF MERIT

In order that the most suitable airfoil for a given aircraft results, it is necessary to direct the design process using some means of quantitatively comparing different candidate airfoils. On first consideration, it might be thought that the airfoil having the highest of the so-called endurance parameter, $c_\ell^{3/2}/c_d$, would offer the best aircraft endurance performance; however, because of the impact of the airfoil on such things as wing area, tail size, and so forth, selection of the airfoil having the highest endurance parameter does not insure that the aircraft will have the highest three-dimensional endurance parameter, $C_L^{3/2}/C_D$. In fact, it was found that in order to maximize the aircraft endurance, the airfoil should be designed such that the figure of merit, given in Fig. 4, is maximized. The figure of merit provides a quantitative means of trading off the gain due to decreasing wetted-area wing drag by increasing the maximum lift coefficient against that of decreasing the section profile-drag coefficient. It should be noted that, if the appropriate operational lift coefficient for which the profile drag is minimized is considered, this figure of merit is the same as that used to design an airfoil for general aviation applications.[1]

- Reduce wing profile drag
  - Decrease wing area by increasing $c_{l,max}$
  - Reduce section profile drag at operational c_l
- Maximize $\left\{ \dfrac{c_{l,max}}{c_d \text{ @ } c_l = 1.5} \right\}$

Figure 4

APPLICATION OF THE FIGURE OF MERIT

As an example of how the figure of merit given in the preceding figure might be used, consider the drag polars of two candidate airfoils as depicted in Fig. 5. The airfoil having performance represented by the solid line has a lower profile-drag coefficient over most of the flight range, while the airfoil represented by the dashed line has a higher maximum lift coefficient which allows the required wing area to be less, and thereby reduces the wetted-area drag. While the two polars are very different, it is entirely possible that the two airfoils have the same maximum section endurance parameters or lift-to-drag ratios. Thus, while it is clear that one of the two must offer better aircraft endurance, it is not at all clear which one it is. The figure of merit, however, provides a quantitative means which allows the proper selection to be made.

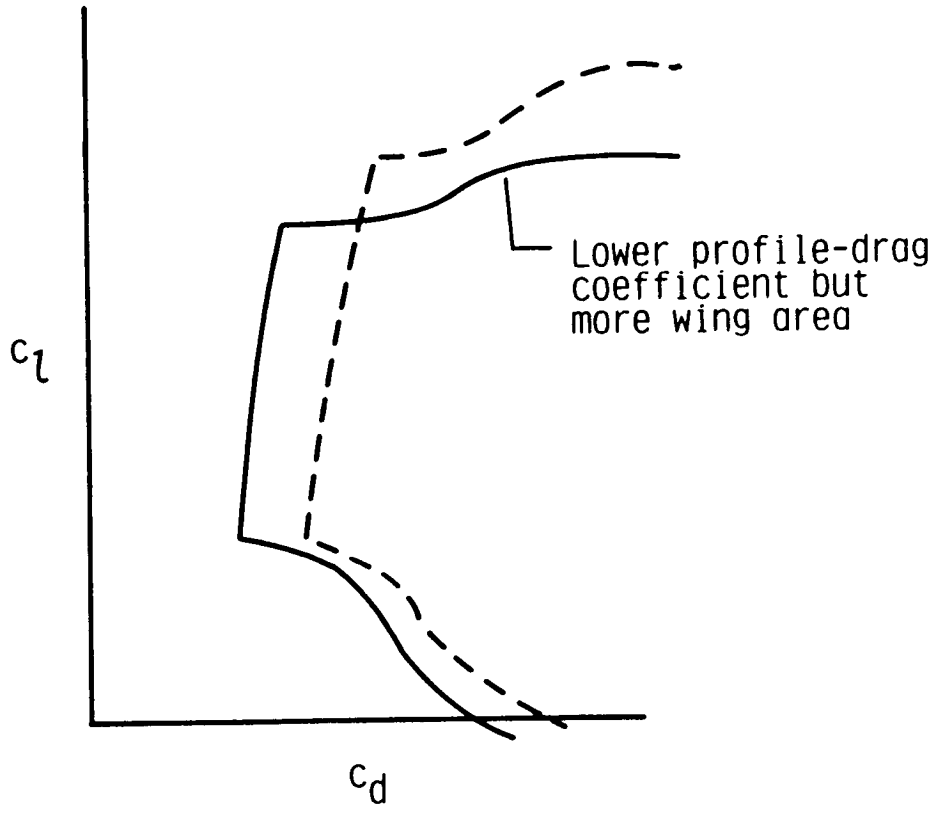

Figure 5

ADDITIONAL DESIGN CONSIDERATIONS

In addition to the design considerations already noted, the constraints indicated in Fig. 6 were imposed. A single-element airfoil was decided on because performance calculations indicated the penalty for carrying the additional weight of a flap system over such a long period of time could not be justified. To keep the trim drag within reasonable limits, it was decided that the airfoil pitching moment coefficient should be no more negative than indicated. Finally, although resulting in a severe limitation on the achievable $c_{\ell,max}$, the constraint was imposed that the maximum lift coefficient should not depend on surface contamination. Thus, take-off and landing performance would be unaffected by rain, bugs, dirt, and so forth, on the wings.

1. No flaps
2. $c_{m,0}$ no more negative than -0.20
3. $c_{l,max} \neq f$(surface contamination)

Figure 6

THE UPPER-SURFACE VELOCITY DISTRIBUTION USED FOR THE ACHIEVEMENT OF $c_{\ell,max}$ INDEPENDENT OF SURFACE CONTAMINATION

In order to achieve $c_{\ell,max}$ independent of surface contamination, the upper-surface velocity distribution was designed to behave as indicated in Fig. 7. The idea is to have the velocity distribution corresponding to $c_\ell = 1.5$, which is the upper limit of the low-drag range, such that the boundary-layer transition is "on the verge" of moving forward from its location just at the start of the main pressure recovery. Thus, for lower angles of attack, the pressure gradients are such that transition will be confined to the ramp just upstream of the main pressure recovery. For higher angles of attack, however, the resulting unfavorable pressure gradients will cause transition to move rapidly toward the leading edge. Thus, the maximum lift coefficient does not depend on a long run of laminar flow. The pressure peaks over the forward portion of the airfoil required to achieve this behavior, however, tend to limit the maximum lift coefficient that can be produced.

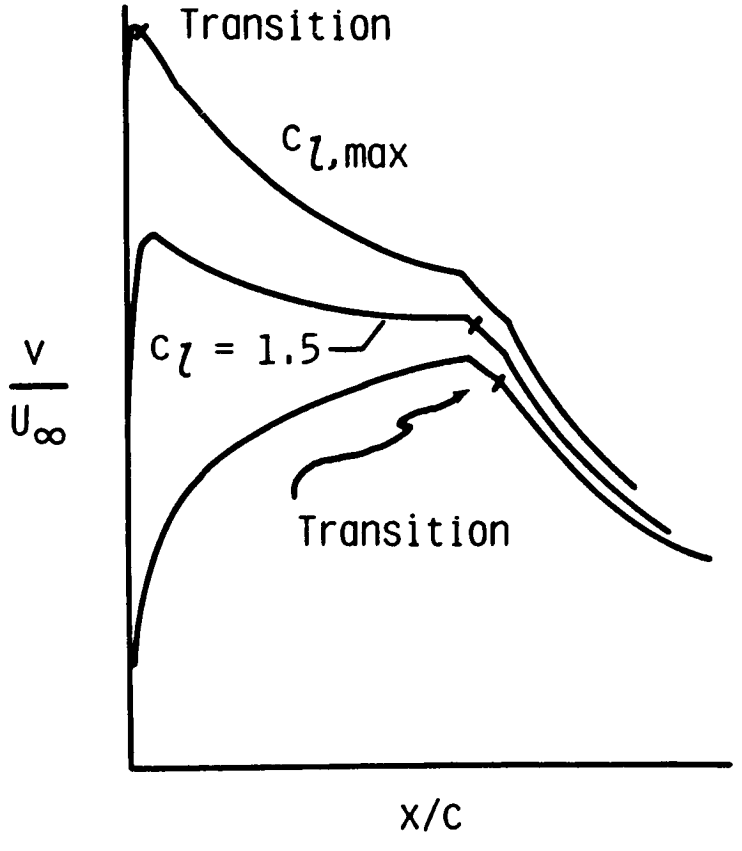

Figure 7

SEPARATION RAMP

In order to operate at the relatively high lift coefficients required by the high-altitude, long endurance mission, the level of the upper-surface velocity distribution must be fairly high. In recovering to free-stream conditions over the aft portion of the airfoil, however, the low operational Reynolds number severely limits the amount of adverse pressure gradient that can be negotiated by the turbulent boundary layer without separation problems. One method of obtaining the lift needed while controlling the extent of upper-surface separation is through the use of the separation ramp (shown in Fig. 8), originally credited to F. X. Wortmann. While some separation is present at angles of attack within the operating range of interest, the ramp limits the amount of separation to less than ten-percent chord. It is not until the angle of attack is near that corresponding to the maximum lift coefficient that the separation point is able to move upstream of the ramp and onto the main pressure recovery.

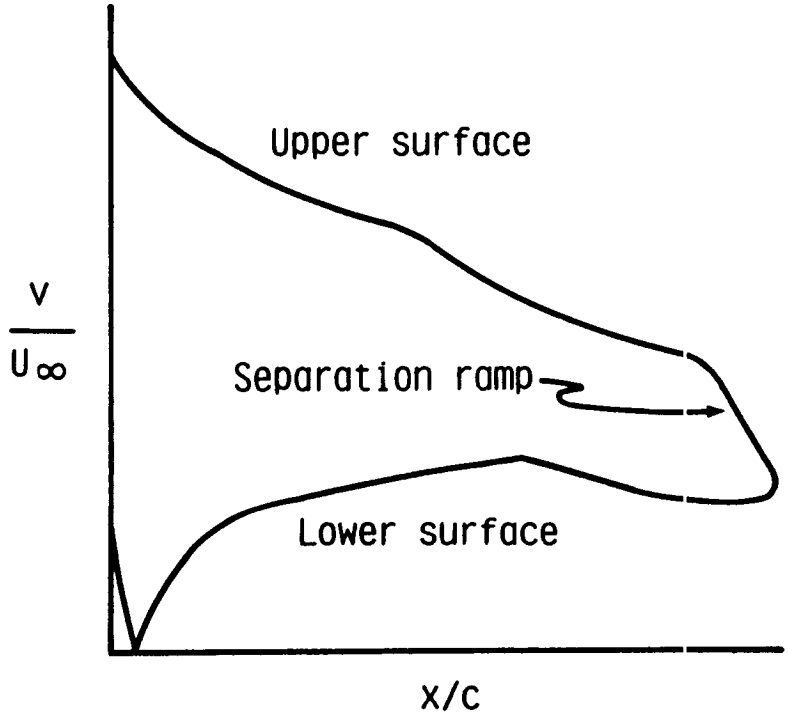

Figure 8

DESIGN METHODOLOGY

Once the design goals were firmly established, the actual design was carried out using the Eppler program.[2,3] Most design methodologies develop the airfoil for a given condition, then explore off-design, and if found unacceptable, modify the design-point solution until acceptable off-design performance is achieved. The Eppler method, however, is unique in that the airfoil is designed to satisfy the entire performance envelope from the onset. This is possible because the method allows different parts of the airfoil to be designed for different operating conditions. For example, as shown in Fig. 9, the upper surface of the airfoil is designed primarily to the upper limit of low-drag range of the polar, corresponding to the high-altitude long-endurance operating point, while the lower surface was designed to the lower limit of the low-drag range, corresponding to the dash requirements.

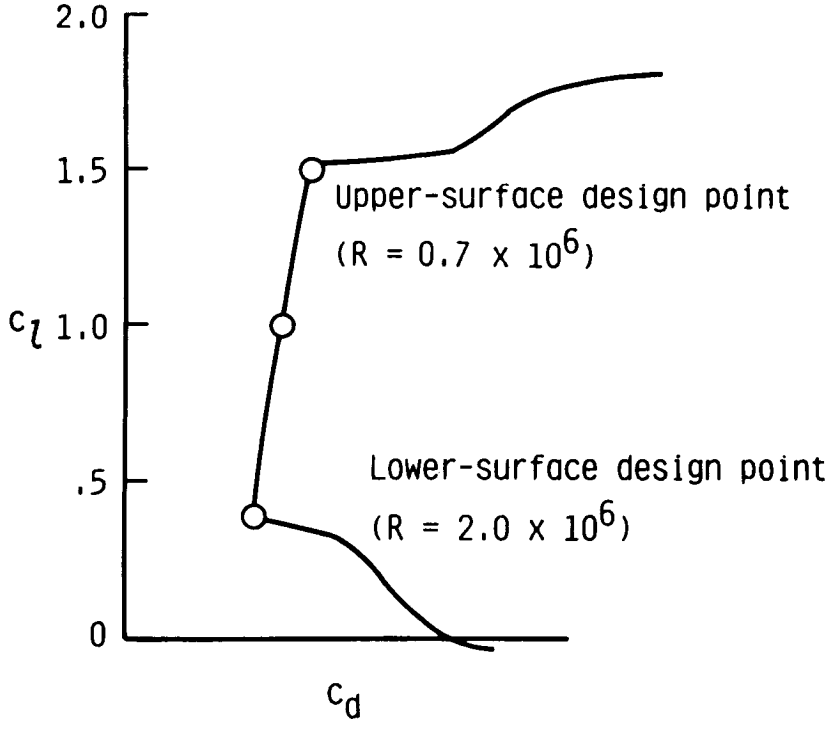

Figure 9

DESIGN FOR DESIRED BOUNDARY-LAYER DEVELOPMENT

It is notable that, unlike most methods which design for a given velocity distribution, the Eppler program makes it possible to go one step beyond this and design an airfoil which achieves a desired boundary-layer development. As an example of the process, consider the program-generated plot, presented in Fig. 10, of Reynolds number based on momentum thickness against the boundary-layer shape factor. Indicated in the figure are the empirically determined criteria for transition and turbulent separation. Also shown for reference are the shape factors corresponding to a laminar separation, stagnation, and the Blasius solution for the boundary layer over a flat plate. The curves plotted in the figure represent the boundary-layer developments at two angles of attack near the upper-surface design condition. Both developments begin at the leading-edge stagnation point and rapidly move toward laminar separation. The development at $\alpha = 14.79$ degrees closely follows the laminar separation criterion and intersects the transition curve at a point on the airfoil corresponding to the start of pressure recovery. The boundary-layer development which is shown for a slightly higher angle of attack intersects the laminar separation line almost immediately, and transition near the leading edge by means of a laminar separation bubble is indicated. This particular development provides for the rapid forward movement of transition for lift coefficients greater than 1.5 and thereby satisfies the requirement that the maximum lift be independent of surface contamination. The desired boundary-layer development on the lower surface is obtained similarly.

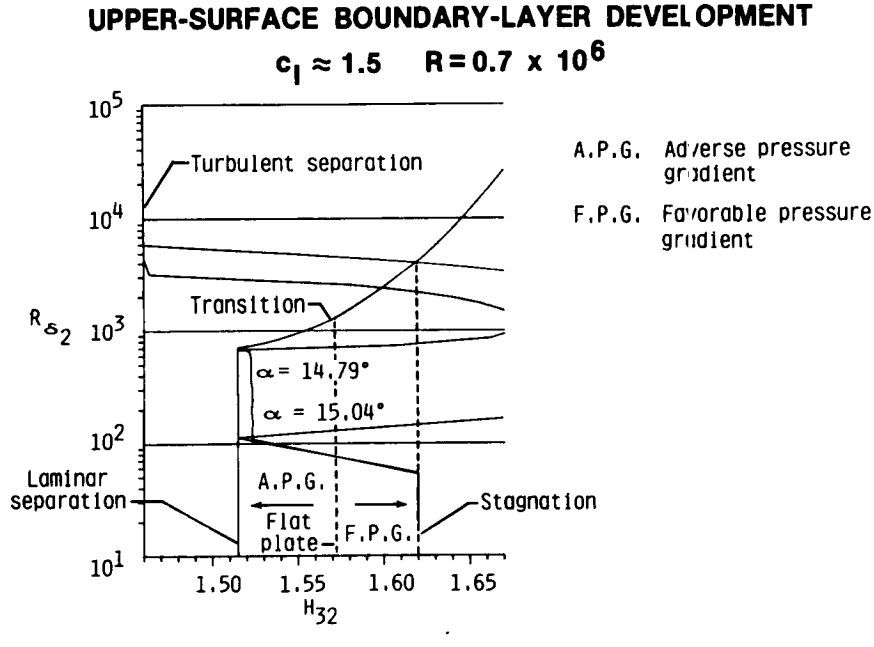

Figure 10

HIGH-ALTITUDE, LONG-ENDURANCE AIRFOIL AND INVISCID VELOCITY DISTRIBUTIONS

The high-altitude, long-endurance airfoil which was designed is presented in Fig. 11. Also included in the figure are the inviscid velocity distributions corresponding to the key design lift coefficients for this airfoil.

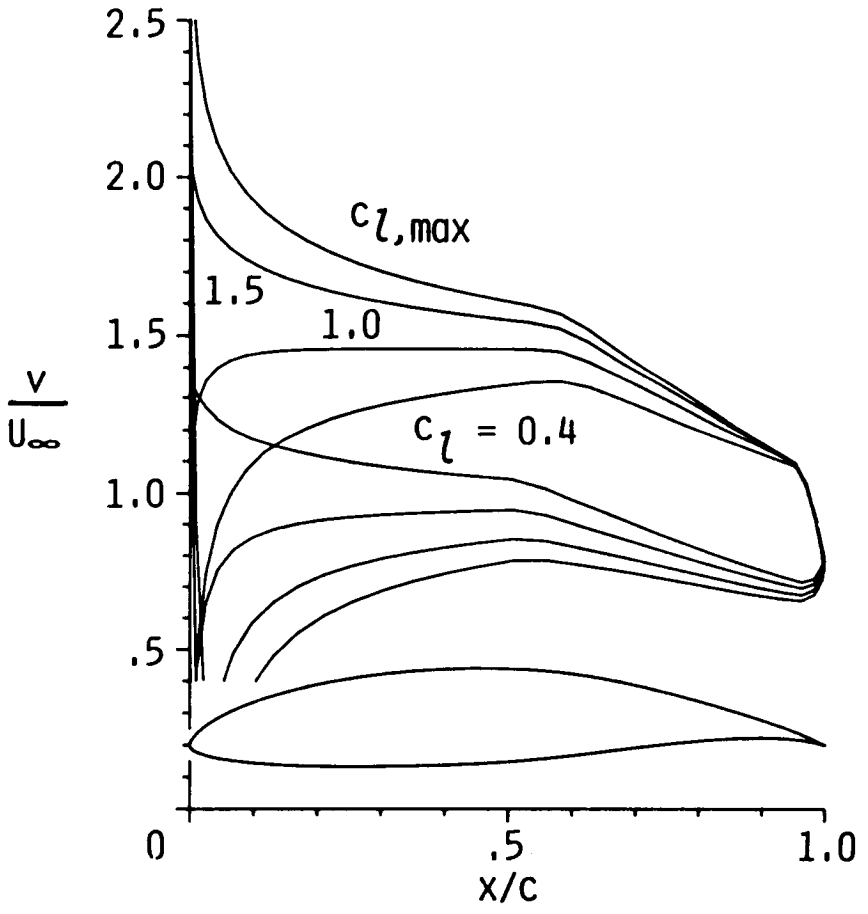

Figure 11

SECTION CHARACTERISTICS
$R = 0.7 \times 10^6$

The performance of the airfoil is summarized in the program-generated plots presented in Fig. 12. The results shown correspond to the long-endurance Reynolds number. Comparing these results with the requirements shown in Fig. 3, it is clear that all the design goals have been satisfied. The small triangles on the drag curves indicate lift coefficients for which a laminar separation bubble is predicted that is significant enough to alter the drag coefficients given. It should be noted, however, that the laminar-separation-bubble warnings occur outside the operating range for the airfoil for this Reynolds number.

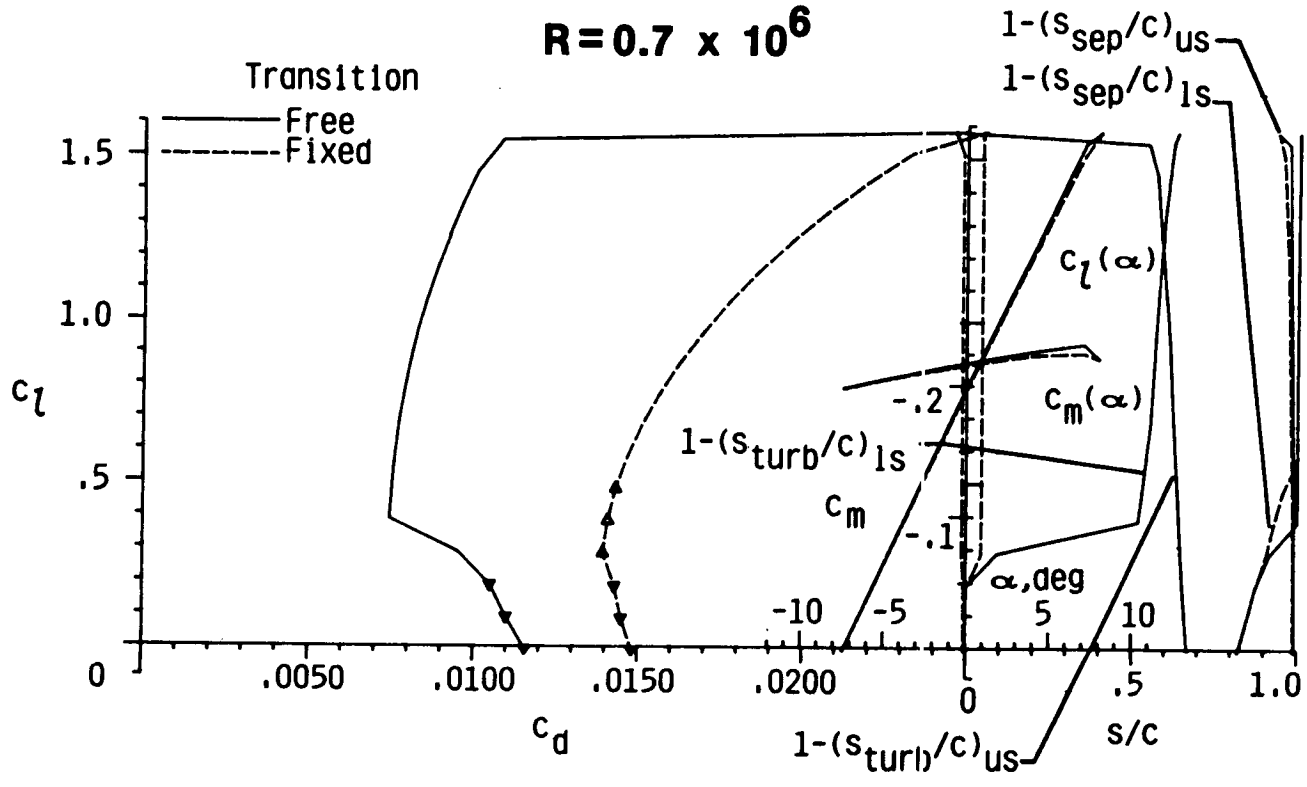

Figure 12

SECTION CHARACTERISTICS
$R = 2 \times 10^6$

The section characteristics for the Reynolds number corresponding to take-off and dash conditions are given in Fig. 13. Of most significance is the fact that the transition-free and transition-fixed polars merge at high lift coefficients. Thus, because the transition point on the upper surface has already moved to the leading edge, the behavior of the airfoil at high lift coefficients is independent of surface contamination which, otherwise, would influence the location of transition. Based on a long-term calibration of the program calculations against wind-tunnel and flight data, a maximum lift coefficient of 1.8 is expected for this airfoil.

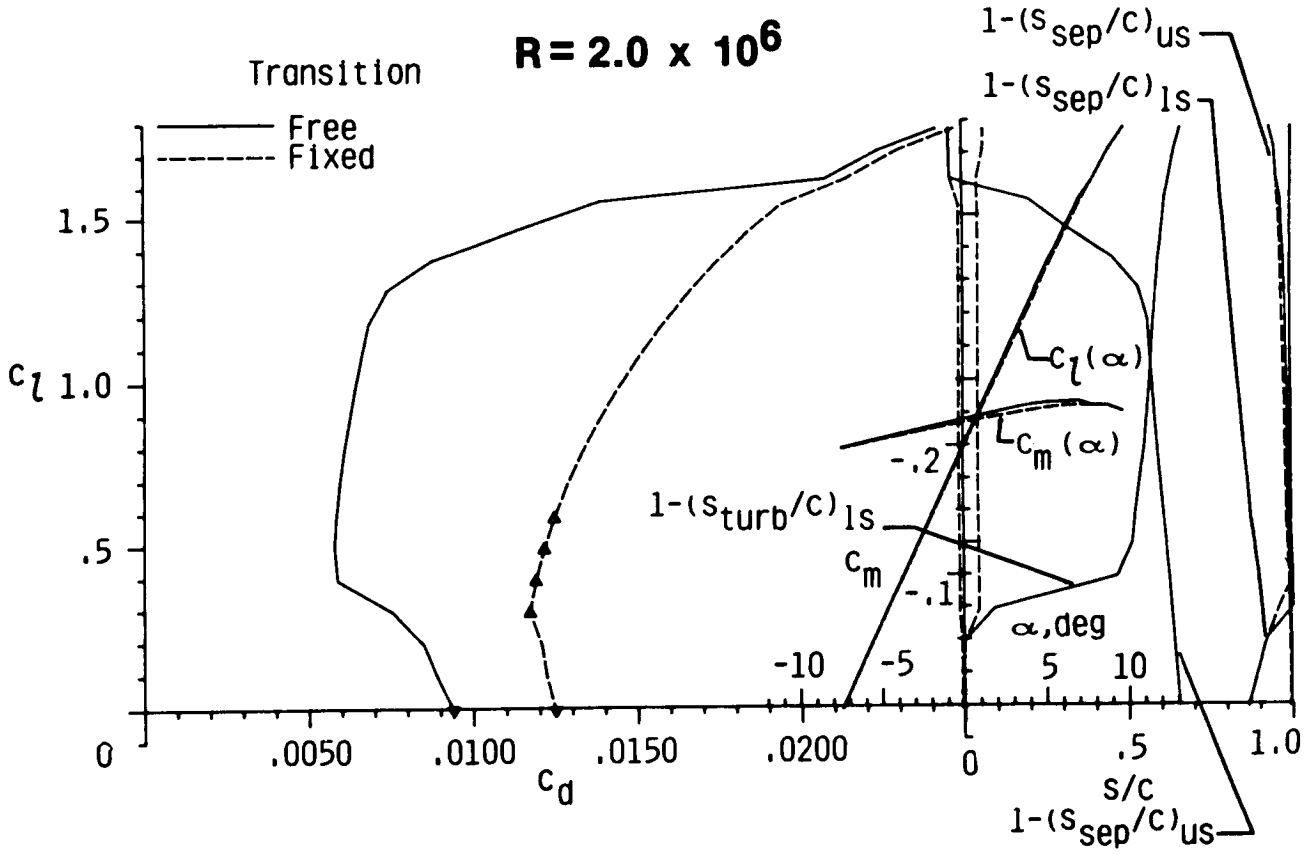

Figure 13

VEHICLE PERFORMANCE COMPARISON

To demonstrate the relative importance of the airfoil performance to that of the overall aircraft, a performance comparison is presented in Fig. 14 for two aircraft which are identical in all respects except for the airfoil utilized on the main wing. The first column results are for the aircraft having an NACA 23015 airfoil, while the second column results are for the vehicle having the new high-altitude, long-endurance airfoil, the NASA NLF(1)-1015. The thirty-percent improvement in endurance and fourteen-percent in range clearly indicate that the potential benefits offered by the new airfoil are significant. While further iteration of the airfoil/aircraft design would result in even better overall performance, the airfoil designed provides realistic, performance data which should facilitate the meaningful preliminary design and sizing of high-altitude, long-endurance remotely piloted vehicles.

	NACA 23015	NLF(1)-1015
Endurance	72 hrs.	93 hrs. (+ 30%)
Range	18,000 mi	21,000 mi (+ 14%)

Figure 14

CONCLUSIONS

The contributions of the airfoil design effort reported in this paper are summarized in Fig. 15.

- Demonstrated importance of integrating airfoil and aircraft designs
- Provided realistic airfoil data to aid future high-altitude, long-endurance aircraft preliminary design
- Developed test case for further validation of Eppler program
- Designed boundary layer -- not pressure distribution or shape
- Achieved substantial improvement in vehicle performance through mission-specific airfoil designed utilizing multipoint capability of Eppler program

Figure 15

SYMBOLS AND ABBREVIATIONS

C_D	drag coefficient
C_L	lift coefficient
c	airfoil chord
c_d	section profile-drag coefficient
c_ℓ	section lift coefficient
c_m	section pitching moment coefficient taken about quarter-chord point
$c_{m,o}$	section quarter-chord pitching-moment coefficient at zero lift
H_{32}	boundary-layer shape factor, δ_3/δ_2
R	Reynolds number based on free-stream conditions and airfoil chord
s	arc length along airfoil surface
s_{sep}	arc length along which boundary layer is separated
s_{turb}	arc length along which boundary layer is turbulent, including s_{sep}
U_∞	free-stream velocity
v	local velocity on airfoil
x	airfoil abscissa
α	angle of attack relative to zero-lift line, deg
δ_2	boundary-layer momentum thickness
δ_3	boundary-layer energy thickness

Abbreviations:

ls	lower surface
us	upper surface

REFERENCES

1. Somers, Dan M.: Design and Experimental Results for a Flapped Natural-Laminar-Flow Airfoil for General Aviation Applications. NASA TP-1865, 1981.

2. Eppler, Richard; and Somers, Dan M.: A Computer Program for the Design and Analysis of Low-Speed Airfoils. NASA TM-80210, 1980.

3. Eppler, Richard; and Somers, Dan M.: Supplement To: A Computer Program for the Design and Analysis of Low-Speed Airfoils. NASA TM-81862, 1980.